



HAL
open science

New high-resolution solar spectrum in the 0.7-1.7 μm domain obtained with the ACS-NIR spectrometer (TGO).

Abdanour Irbah, Jean-Loup Bertaux, Franck Montmessin, Alexander V. Trokhimovskiy, Oleg I. Korablev, Anna A. Fedorova

► To cite this version:

Abdanour Irbah, Jean-Loup Bertaux, Franck Montmessin, Alexander V. Trokhimovskiy, Oleg I. Korablev, et al.. New high-resolution solar spectrum in the 0.7-1.7 μm domain obtained with the ACS-NIR spectrometer (TGO).. Space Telescopes and Instrumentation 2024: Optical, Infrared, and Millimeter Wave. Proceedings SPIE 13092, SPIE, Jun 2024, Yokohama, Japan. Paper 13092-218. insu-04626267

HAL Id: insu-04626267

<https://insu.hal.science/insu-04626267v1>

Submitted on 10 Sep 2024

HAL is a multi-disciplinary open access archive for the deposit and dissemination of scientific research documents, whether they are published or not. The documents may come from teaching and research institutions in France or abroad, or from public or private research centers.

L'archive ouverte pluridisciplinaire **HAL**, est destinée au dépôt et à la diffusion de documents scientifiques de niveau recherche, publiés ou non, émanant des établissements d'enseignement et de recherche français ou étrangers, des laboratoires publics ou privés.

New high-resolution solar spectrum in the 0.7-1.7 μm domain obtained with the ACS-NIR spectrometer (TGO)

Abdanour Irbah^a, Jean-Loup Bertaux^a, Franck Montmessin^a, Alexander Trokhimovskiy^b, Oleg Korablev^b, and Anna Fedorova^b

^aLATMOS/IPSL, UVSQ Université Paris-Saclay, Sorbonne Université, 11 BD D'Alembert, 78280 Guyancourt, France

^bSpace Research Institute (IKI), 84/32 Profsoyuznaya, 117997 Moscow, Russia

ABSTRACT

The infrared solar spectrum measured from the ground is difficult, if not impossible, outside the observation windows permitted by the Earth's atmosphere. Existing solutions then call on modelling of the Sun, correction of ground measurements of atmospheric transmission or even measurements from space. This latter opportunity was seized with infrared observations from the Trace Gas Orbiter (TGO) interplanetary probe orbiting MARS launched to study its atmosphere using spectrometers installed on its Atmospheric Chemistry Suite (ACS) platform. The spectrometer ACS-NIR (Near InfraRed) thus makes it possible to probe the Martian atmosphere in the 0.7-1.7 μm spectral domain thanks to its solar occultation mode. In this mode, the ACS-NIR is pointed toward the Sun and its line of sight gradually passes through MARS' atmosphere as the satellite moves in its orbit. The high-resolution solar spectrum is directly measured when the line of sight is above the atmosphere. A 10-month observation plan (October 2020-August 2021) consisting of recording all diffraction orders from the ACS-NIR was specifically deployed for this objective. One of the main concerns we face when recovering the solar spectrum is spectral contamination of diffraction orders. We will first present how we processed the diffraction order images to obtain the best possible solar spectrum in the 0.7-1.7 μm band. We will show how the use of 3 off-centre images of the same diffraction order allows both to avoid spectral contamination and to improve the detection of solar lines at the ends of the order image where the intensity is low. We will then show the final version of the solar spectrum that we obtain which will be compared to the Toon spectrum taken as a reference. We will finish by addressing the parts of the spectrum which present solar lines located in spectral bands not observable from Earth and absent from the reference spectrum.

Keywords: Solar spectrum, Near Infrared, Mars, Spectrometer, AOTF

1. INTRODUCTION

The main information that comes from the Sun is its radiation, which is very useful for us to know its chemical composition and to understand how it works. Its energy distribution with the wavelength thus defines the solar spectrum which is very close to that of a black body at the temperature of approximately 5800 K. The spectrum of the black body varies continuously with the wavelength whereas that of the Sun presents many absorption lines. They are due to the elements of the cold layer above the photosphere which absorbs radiation coming from the lower layers.¹ The solar spectrum therefore informs us about the elements that make up the Sun but also about its magnetic field which impacts certain solar lines. The solar spectrum can be obtained from a theoretical approach, from ground/balloon measurements after subtraction of telluric lines like G. Toon did,² or from measurements outside any atmosphere, i.e. from space. The latter is known as the exo-atmospheric method and is used in this work. The measurements to obtain the solar spectrum were carried out with the Near InfraRed spectrometer (NIR) installed on the Atmospheric Chemistry Suite (ACS) platform on board the Trace Gas Orbiter (TGO) launched in 2016 and still operational today.³ Indeed, the ACS-NIR spectrometer makes it possible to obtain high-resolution spectral bands from diffraction orders thanks to its resolving power of $\sim 25,000$.

Further author information: (Send correspondence to Abdanour Irbah)
A.A.A.: E-mail: air@latmos.ipsl.fr, Telephone: +33 (0)1 8028 5040

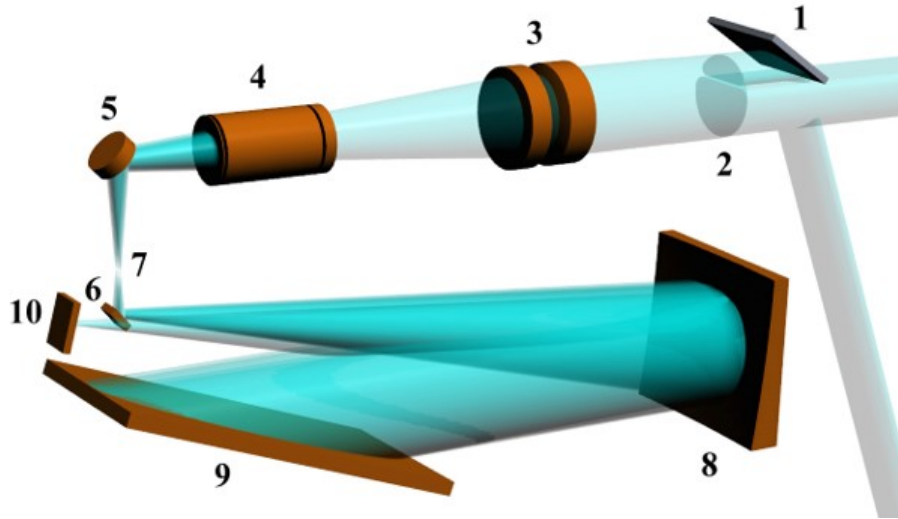


Figure 1. Optical scheme of the spectrometer ACS-NIR reproduced courtesy TGO-ACS.
 1- solar FOV telescope 2- blocking filter 3- entry telescope 4- AOTF in the converging beam
 5, 6- folding mirrors 7- slit 8- main collimating mirror of the spectrometer 9- diffraction grating
 10- detector array

The measurements are carried out for this with its Solar Occultation (SO) mode used nominally to probe the atmosphere of Mars. The spectral signature of atmospheric components present on the line of sight (LOS) is detected in this mode when ACS-NIR points the Sun through the atmosphere of Mars. The solar spectrum is then directly measured when the LOS is above the atmosphere. Special observations were specifically carried out with ACS-NIR to construct the solar spectrum in the range it allows, namely 0.7-1.7 μm . They consisted of acquiring all of the ACS-NIR diffraction orders over a period of approximately 10 months. The spectral bands of successive orders can, however, overlap, giving rise to *spectral contamination*.⁴ The consequences are a pollution of the spectral bands of the diffraction orders by wavelengths coming from their neighbors.

The main objective of this paper is to present how we processed the diffraction order images to obtain the best possible solar spectrum in the 0.7-1.7 μm domain. The method presented uses 3 off-center images of the same diffraction order, which makes it possible both to avoid spectral contamination and to improve the detection of solar lines at the ends of the order images. The final version of the solar spectrum obtained is then compared to the Toon's spectrum taken as a reference. The parts of the spectrum which present solar lines located in spectral bands difficult to access from Earth and absent from the reference spectrum are finally presented.

2. THE ACS-NIR SPECTROMETER AND ORDER DATA CALIBRATION

We will begin by recalling how the ACS-NIR spectrometer works, the different calibrations of the images it provides and the dataset that was constructed to obtain the solar spectrum.

2.1 The ACS-NIR spectrometer

The spectrometer ACS-NIR is a combination of an echelle spectrometer and an Acousto-Optic Tunable Filters (AOTF), which makes it possible to select the different diffraction orders and thus to obtain a high spectral resolution thanks to this set.³ The AOTF controls the wavelength of the diffracted light passing through it thanks to the frequency of the acoustic oscillation causing the crystal of which it is composed to vibrate. Figure 1 shows a simplified optical scheme of the spectrometer ACS-NIR. The spectrometer slit allows selection of a narrow portion of the solar image formed through the AOTF and the corresponding light is diffracted by the grating. The diffraction orders are then imaged on the detector (an infrared camera module XSW-640 from Xenics based on a thermo-electrically cooled (Peltier element) InGaAs array of 640 x 512 pixels) and stored.

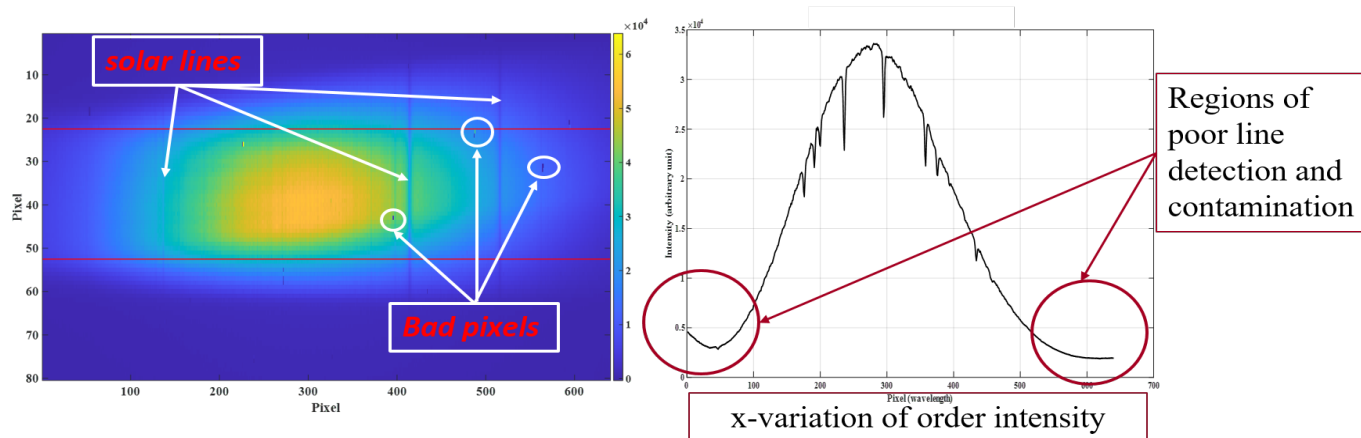


Figure 2. Left: a typical image of the spectrometer ACS-NIR corresponding to the diffraction order 73. Right: variation of the intensity profile on the x-axis passing through the photo-center ordinate of the order image.

The left panel of Figure 2 shows a typical diffraction order image where the solar lines are clearly visible (dark vertical lines) as well as bad pixels (cosmic rays, detector defects...). The red lines delimit the Sun size.

2.2 Operation mode and calibration data

2.2.1 The data acquisition process

Several diffraction orders are acquired sequentially during observations. They can be located anywhere in the entire spectral domain of the instrument thanks to the frequency tuning of the AOTF. Thus, the data acquisition process consists in acquiring all the ACS-NIR diffraction orders used to construct the solar spectrum over the spectral domain 0.7-1.7 μm but also to carry out spectrometer calibration studies. They are obtained by continuously varying the AOTF frequency, giving rise to the dataset called calibration data. However, the main disadvantage of the optical design is the narrowness of the selected spectral intervals. Adjacent diffraction orders can then superimpose on top of each other resulting in a spectral contamination.³ Furthermore, the echelle grating efficiency quickly decreases away from the Blaze angle (centre of the detector) and induces a significant reduction of signal near the edges of the detector³ (see Fig. 2 right panel). These disadvantages will then require the use of specific data processing to overcome them.

2.2.2 The calibration data

The calibration data corresponds to the series of special observations recorded with ACS-NIR pointing at the Sun with its LOS above the Martian atmosphere. They were acquired during 3742 orbits between October 4, 2020 and August 6, 2021 (10 months). The data corresponds to images of all ACS-NIR diffraction orders whose numbers vary from 45 to 103. They were obtained by varying the AOTF frequency from 64 to 156.9 MHz (authorized band) by step of 100 KHz. About 16 files of 34 images are generated for each diffraction order except for orders 45 and 103, which have fewer files due to AOTF frequency limits: they are therefore less well defined. There are 31280 images in total which cover the entire spectral domain of the instrument, from 0.7 to 1.7 μm . Each order image has a size 80 x 640 pixels (see Fig. 2 right left) corresponding to a window extracted from the entire image of size 512 x 640 pixels.

The raw images of the diffraction orders must be corrected of bad pixels, the flat field and the stray light of the spectrometer ACS-NIR. The correction of bad pixels is easily done by the combined action of a median filtering followed by a threshold detection. Corrections of flat fields and stray light images require the development of appropriate methods because they are not provided with data to be processed. These methods have already been developed and well presented in previous published work.^{4,5}

Obtaining the flat field and stray light images is briefly here after.

The flat field matrix corrects the intensity response of the detector pixels, i.e. the pixel response to uniform

illumination. The idea to estimate it is to average all images in the calibration dataset (31,280 images). This average will scramble the solar lines because each diffraction order is formed on the same part of the detector while the solar lines present inside are in different places from one order to another. The average image without traces of solar lines contains the flat field carried by 2D intensity variations similar to those in the image in Figure 2 on the left. The final flat field image is then corrected for 2D intensity variations thanks to a polynomial fit of order 6. The resulting flat field exhibits residual fluctuations at the center with a standard deviation of about 1.2% and about 1.7% at the ends of the diffraction order where the intensity is low.

The stray light matrix of the photometer is also estimated from ACS-NIR observations using the method detailed in irbah *et al.* (2022).⁵ A simulation was first carried out to explain the shape of the solar limb i.e. solar intensity variation along its diameters. Here It corresponds to a section taken in the average image of all diffraction orders along the the ordinate axis (y-axis). The Hestroffer and Magnan’s solar limb model⁶ is used to simulate images at the AOTF output. It was shown in the previous reference that the AOTF is responsible for the shape of the average image and that stray light can be estimated from the intensity at the ends of the limbs. The intensity level of the stray light was found equal to about 6.7% compared to that of the average image.

2.3 Spectral calibration of diffraction orders and the Toon’s spectrum reference

Spectral calibration of the diffraction orders is possible thanks to the *grating dispersion law* and a *reference spectrum*. The dispersion law expresses the relationship between the wavelengths of the diffraction order and its number. It is written as follows:

$\lambda \cdot n = constant$ where λ and n denote the wavelength and the order number respectively.

We consider an ACS-NIR diffraction order containing strong solar lines. The identification of solar lines with a reference spectrum then allows the spectral calibration of the diffraction order considered. A vector of 640 constants where 640 corresponds to the size of the order images along the x-axis, is calculated from the calibrated order and its number using the dispersion law. The spectral calibration of all diffraction orders is immediately deduced from this vector and the order numbers.

The spectrum of G. Toon^{2,7} is used for calibration operations but also taken as a reference to compare that which will be obtained with ACS-NIR. It is a solar pseudo-transmittance spectrum obtained from real spectra recorded from the ground and from balloons from which telluric absorption lines are discriminated using HITRAN (high-resolution transmission molecular absorption).⁸ Toon uses a telluric subtraction method to differentiate between solar and telluric absorptions. It consists of using a variety of solar spectra obtained under low air mass conditions and measured under different conditions (central zone of the Sun or entire disk). Next, it fits the calculated telluric transmission spectrum and then divides each measured spectrum by the adjusted atmospheric transmission. Solar *pseudo-transmittances* have values between 0 and 1⁷ where the upper value (1) corresponds to the solar continuum. The Toon’s spectrum has a very high resolution. It is therefore convolved with a Gaussian function in order to have the same resolution as that of ACS-NIR, which has a resolving power ($\frac{\lambda}{\Delta\lambda}$) of around 25000.³ Figure 3 shows the Toon solar pseudo-transmittance spectrum. It is set to the same spectral sampling as that of ACS-NIR.

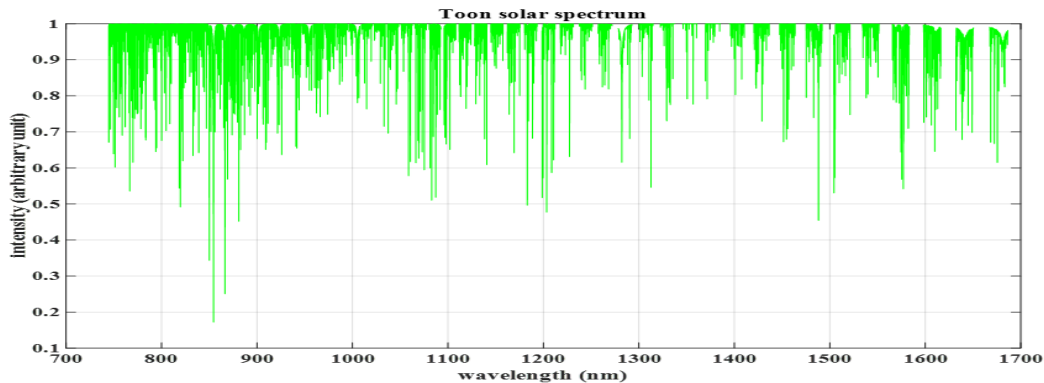


Figure 3. The Toon’s solar pseudo-transmittance spectrum taken as a reference: it is resampled like that of ACS-NIR.

3. DATA PROCESSING TO BUILD THE SOLAR SPECTRUM

We have presented in recent articles a geometric method allowing to obtain the spectral bands without contamination from the images of the diffraction orders of ACS-NIR⁴ and the method to obtain the spectral contamination matrix of the spectrometer.⁹ The main steps of the geometric method are first recalled then how the spectral contamination matrix is obtained.

3.1 The geometric method to avoid spectral contamination

The first step is to extract the spectral band from a diffraction order image corrected beforehand from the bad pixels, flat field and stray light (see Section 2.2.2). It is then necessary to choose the region of the Sun whose spectrum is sought (center, edge, entire disk). The white lines in Figure 4 at the top left delimit the area chosen in the image which here corresponds to the whole Sun. The spectral band is then obtained by integrating in this region the intensity of the order image along the y-axis (see Figure 4 bottom left). Solar lines are clearly visible in this spectral band. They are carried by a continuum which presents a low frequency variation along the wavelength axis. The spectral band extraction process is then applied to all ACS-NIR diffraction orders. The result is presented in the form of an image in Figure 4 on the right. Each line in the image corresponds to a spectral band associated with the AOTF frequency which made it possible to acquire the diffraction order. The order 45 corresponding to the lower limit permitted from the AOTF frequency is located at the bottom of the figure while the order 103 is at the top and corresponds to the upper limit of permitted AOTF frequency. We are now faced with two main concerns in the construction of the solar spectrum which are the spectral disentangling of successive orders and the correction of intensity variations of the continuum of orders (see Section 2.2.1).

The first concern arises essentially at low infrared wavelengths, i.e. for diffraction orders with large numbers, in particular when operating at a fixed AOTF frequency as in the ACS-NIR nominal mode. Figure 5 (top left) is a zoom of Figure 4 (right panel) around large order numbers where white straight lines correspond to AOTF frequencies. There is an obvious drift in the wavelength (pixel axis) of the orders when the AOTF frequency changes. Two or more orders can then be affected by the same AOTF frequency. This can be clearly seen in the intensity profiles in Figure 5 (top right) which are fixed frequency slices taken in the image of order spectral bands plotted in the frame [pixel (wavelength), frequency]. It is then necessary to take oblique slices in the spectral band image following the frequency-wavelength drift (Figure 5 at the bottom left). The solar lines of the considered diffraction order are then in their correct locations, as shown by the plot of the intensity profiles in Figure 5 at the bottom right. However, only a few intensity profiles located in the area around the maximum intensity of the diffraction order are taken in order to avoid contamination of neighbors (red straight lines in the Figure 6 on the left). The average profile is then calculated and shown in black in Figure 6 on the right. It exhibits variations in intensity with wavelength as expected and this is now the subject of a second concern.

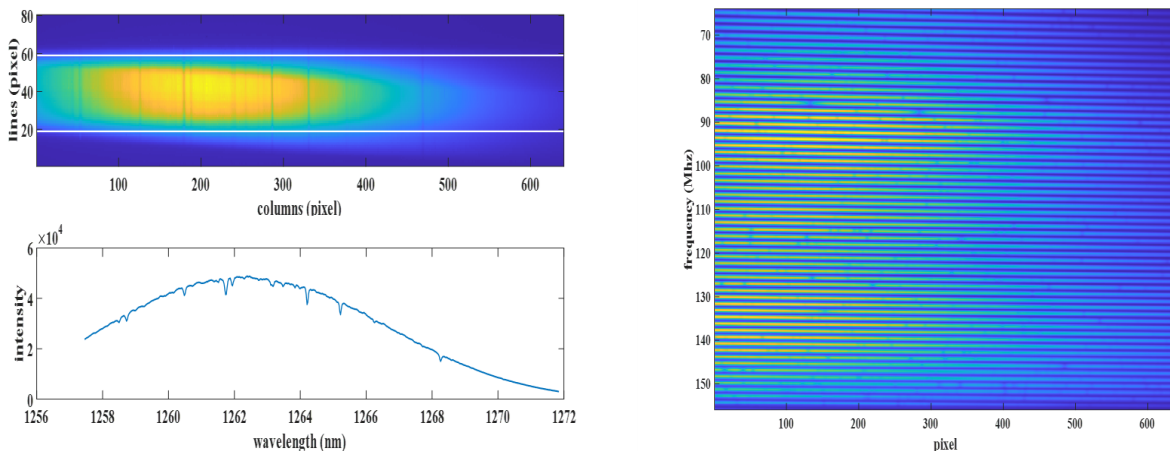


Figure 4. Left: Extraction of the order spectral bands. Right: All extracted spectral bands from ACS-NIR order images.

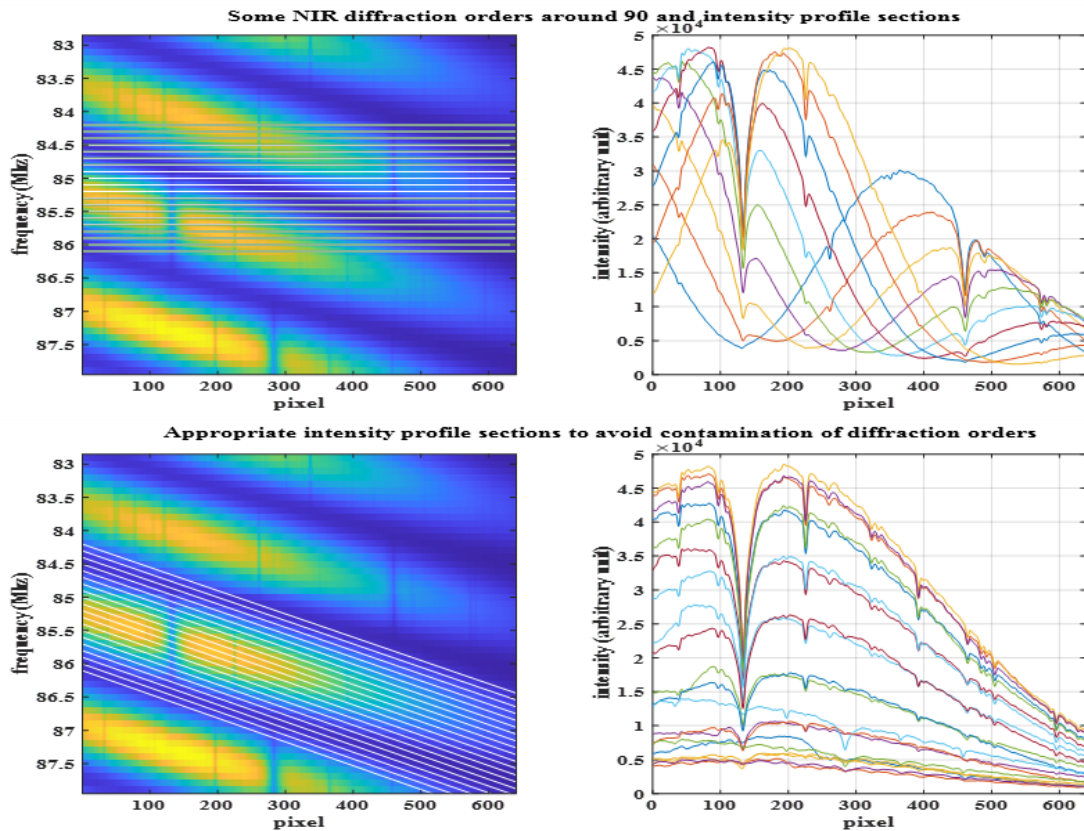


Figure 5. Left: Extraction of the order spectral bands. Right: Extracted spectral bands from corresponding order images.

The average profile of each diffraction order is well fitted with a Blaze function.⁴ Figure 7 (top) plots the average profile of order 94 and its approximation with a Blaze function. This approximation is then used to correct for the low-frequency intensity variation of the average profile and the result shown in Figure 7 (middle). This plot reveals that the continuum is arbitrarily set to 1 by this operation and that certain residual oscillations remain. Thus, the envelope defined by the local extrema of the fluctuations is detected (red curve in the figure) and used to reduce the residual fluctuations. The final result shown in Figure 7 (bottom) is then the spectral band of the

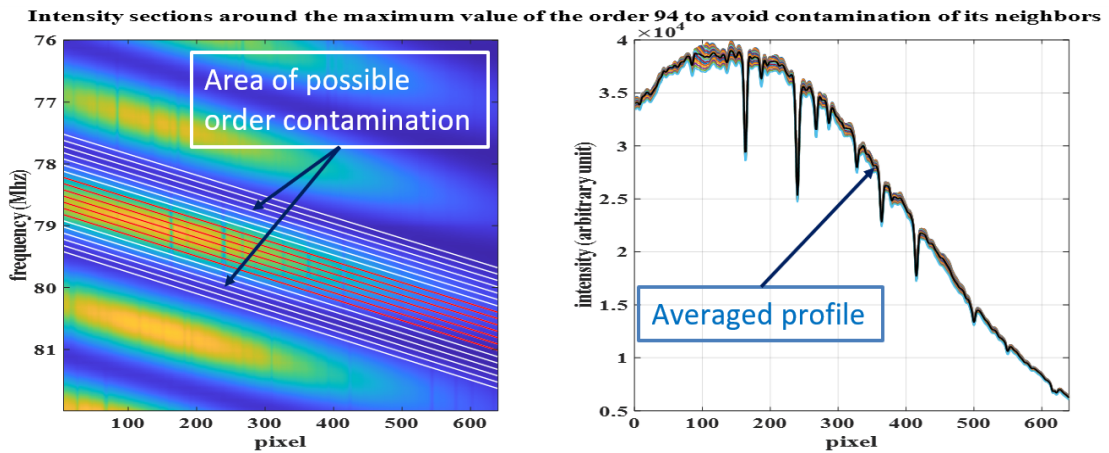


Figure 6. Intensity profiles to avoid contamination (left) then calculation of the average profile (right).

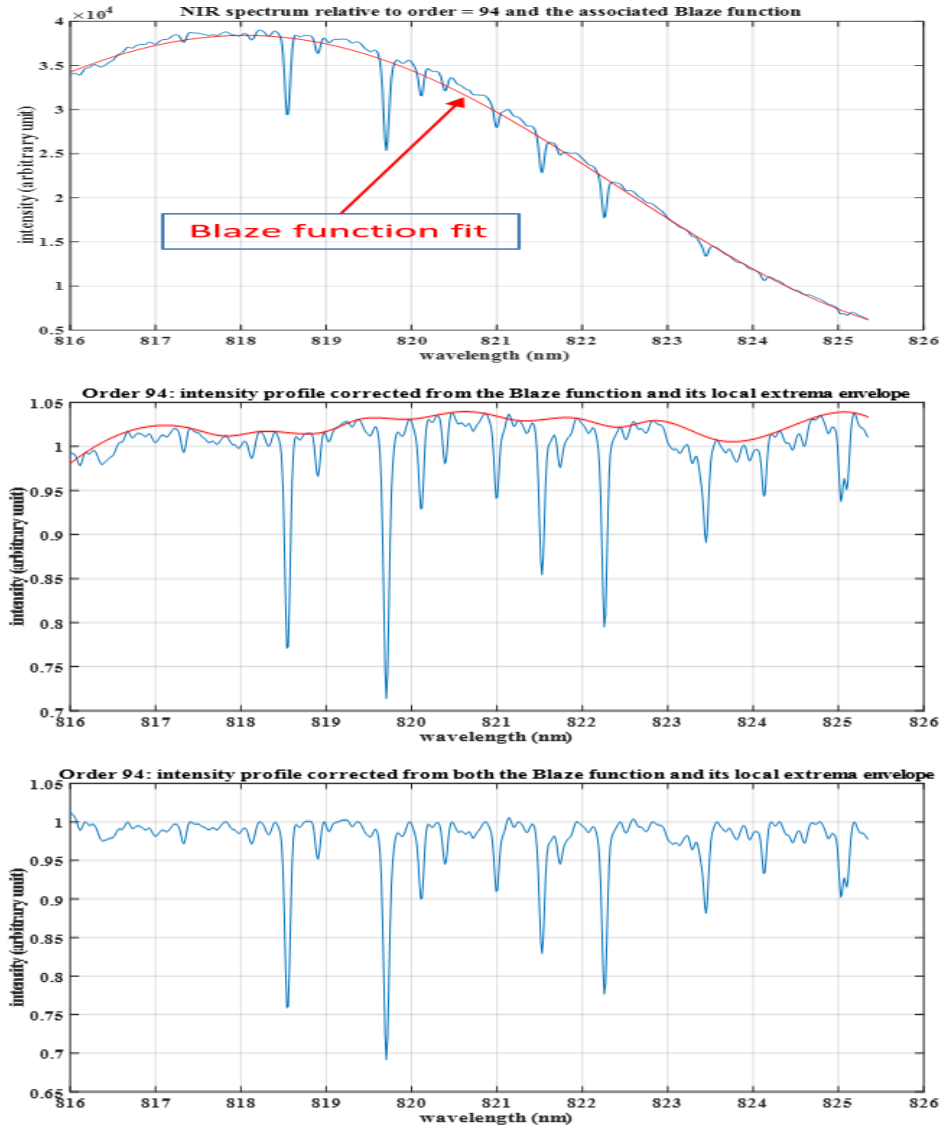


Figure 7. Top: Average profile of order 94 fitted with a Blaze function. Middle: Average profile corrected with Blaze function fit but residual oscillations remain. Bottom: Oscillation corrections and the final order spectral band

diffraction order considered (94).

At this stage, all the average intensity profiles obtained from the ACS-NIR diffraction orders can be processed according to the method presented above in order to construct the solar spectrum over the 0.7-1.7 μm range which will correspond to the region of the Sun considered, here the entire Sun (see Figure 4 at the top left).

3.2 The contamination matrix

If the ACS-NIR solar spectrum can at this stage be constructed from the calibration data, it nevertheless remains disturbed by the filtering introduced during the extraction of the oblique slices in the image of the order spectral bands. The same goes for the poor estimation of the solar lines at the ends of the orders where the intensity is low. Thus, the geometric method does not provide a correct solution for the solar spectrum. More generally, ACS-NIR observations carried out in nominal operating mode to probe the Martian atmosphere require the acquisition of selected diffraction orders linked to fixed AOTF frequencies. This can therefore lead to spectral contamination by adjacent orders, particularly when acquiring diffraction orders with high numbers. Better

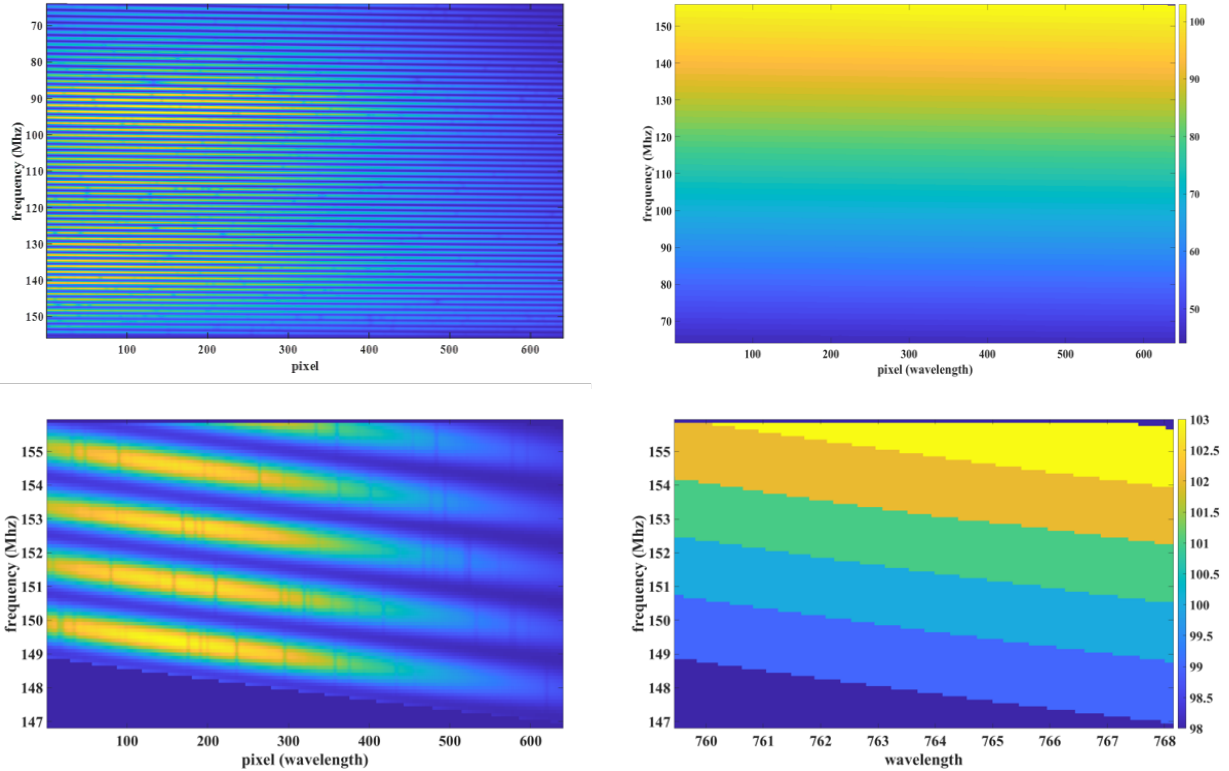


Figure 8. Top: spectral bands obtained from diffraction orders (left) - The spectral contamination matrix (right). Bottom: zoom around the spectral band of order 101 (left) and the corresponding part of the spectral calibration matrix (right).

knowledge of contamination between diffraction orders is therefore necessary before considering solutions to these problems that arise.

The study of order spectral contamination can be carried out using the geometric method with calibration data which allows obtaining a version of the solar spectrum without contamination. Indeed, the spectral contamination matrix of the spectrometer ACS-NIR can be deduced if we encode each spectral band of the diffraction orders with their number. Figure 8 at the top left repeats the left image of Figure 4, which shows all the spectral bands obtained from the orders. The spectral contamination matrix obtained when the spectral bands are encoded with order numbers ranging from 45 to 103 is shown at the top right in the figure. A zoom on these two images is carried out around order 101 with 2 adjacent orders on either side. It is shown respectively on the 2 lower images in order to better appreciate the coding of the diffraction orders. The diffraction order 101 and its 2 neighbors, top and bottom, are taken as an example since the entanglement between orders is almost certain. It will be considered below to illustrate how the spectral contamination matrix is used.

The case of fixed AOTF frequencies is considered. Horizontal slices are then extracted from the encoded image of the order spectral bands. They are represented by red lines in Figure 9 on the left which zooms in on order 101. This figure clearly shows that the same line, i.e. a fixed AOTF frequency, crossing order 101 also intercepts diffraction orders 100 and 102. Figure 9 on the right shows all profiles extracted from the encoded image that correspond to the chosen frequencies (horizontal red lines). The dark line in the figure is the AOTF frequency which clearly minimizes inter-order contamination. Indeed, this frequency is the one which among all gives the maximum number of pixels defining the order considered (101) and minimizes those of adjacent orders (100 and 102). This frequency will be used in nominal mode when acquiring this diffraction order of interest.

The illustration with order 101 clearly shows how the spectral contamination matrix can be used to know how a given order spectral band linked to a fixed AOTF frequency is affected by wavelengths coming from neighboring orders.

We will now see in the following section how the use of only a few images makes it possible to overcome both the

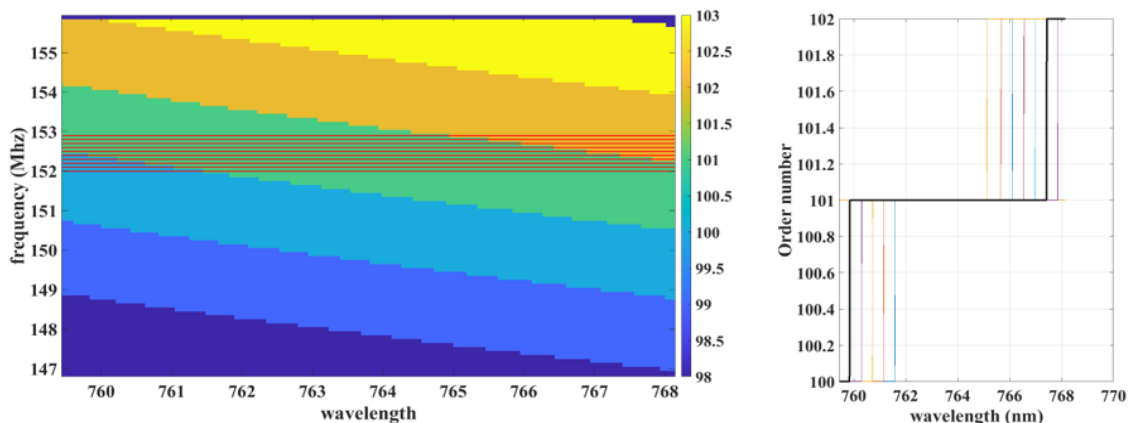


Figure 9. Left: image of the encoded spectral band close to order 101 and fixed AOTF frequencies (horizontal red lines). Right: contamination of the corresponding profiles in case of fixed AOTF frequencies. The dark line is the AOTF frequency which minimizes inter-order contamination.

contamination between adjacent diffraction orders and the poor detection of solar rays at the ends of the order where the intensity is weak.

4. THE SOLAR SPECTRUM: NEW METHOD AND RESULTS

The geometric method using the ACS-NIR calibration dataset makes it possible to construct a solar spectrum without spectral contamination but with certain limitations. The spectral contamination matrix of diffraction orders related to the spectrometer was also established using this method and calibration data. This allows us to know how a diffraction order is contaminated by its immediate neighbors and to now consider new perspectives for constructing a better quality solar spectrum.

4.1 Obtaining spectral bands of ACS-NIR diffraction orders without contamination

The evolution of a given diffraction order can be followed using calibration data, i.e. follow its evolution towards the next one, thanks to the continuous variation of the AOTF frequency in small steps of 0.1 MHz. Thus, each ACS-NIR diffraction order will appear at a certain AOTF frequency, which will result in its truncated image on the detector. The diffraction order will then increase as the AOTF frequency increases to reach its maximum size providing the complete image on the detector. Its size will then decrease when the AOTF frequency continues to increase to again give a truncated image on the detector but formed opposite to that of its appearance. We will take advantage of this change in size of the diffraction order to better reconstruct it while avoiding any spectral contamination. Indeed, we know how it is contaminated at each stage of its evolution thanks to the spectral contamination matrix. This is the basis of the new method that we will put into practice to construct the solar spectrum.

Three off-center images of the same order obtained with three different AOTF frequencies are first required. They will be split to then reconstitute the spectral band of the chosen order. The contamination matrix helps to find the best candidates in the series giving the order evolution with the AOTF frequency i.e. images of the order which will give maximum intensity to the ends of the diffraction order which will be built by assembly. Indeed, a part without spectral contamination will be extracted from each image thanks to the contamination matrix, then used for the reconstruction of the spectral band of the diffraction order. Figure 10 shows the three selected images that will be used to reconstruct the spectral band of diffraction order 101, which is again taken as an example to illustrate the method. These images shown in the top, middle, and bottom panels of the figure were obtained with AOTF frequencies of 153.4, 152.3, and 151.5 MHz, respectively. The diffraction order image acquired at the frequency 153.4 MHz will be used to obtain the left part of the spectral band and those taken

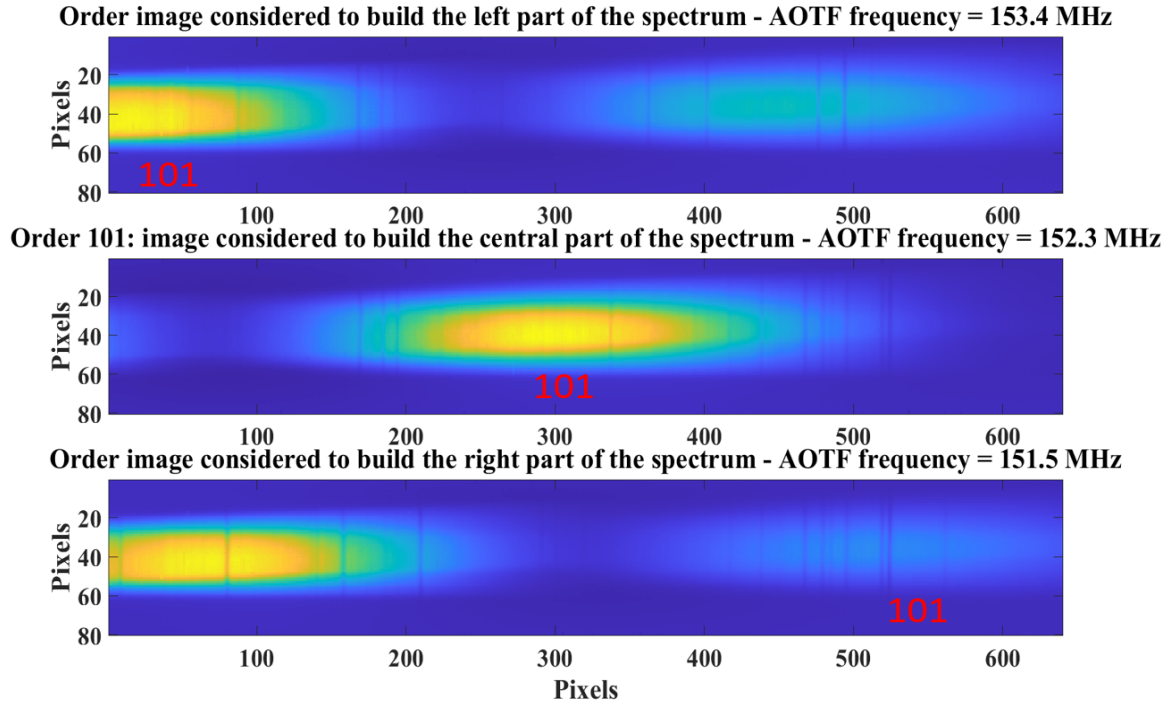


Figure 10. Three images of the same diffraction order (number 101) obtained with different AOTF frequencies: they are used to build the recombined spectral band.

at 152.3 and 151.5 MHz for the middle and right parts respectively. This is clearly visible in Figure 11 at the top where the spectral bands of the images acquired at 153.4, 152.3 and 151.5 MHz are plotted in blue, red and green respectively. They were calculated considering the whole Sun as an integration region (see Section 3.1). We see in the figure that the intensity level at the start of the blue curve is high, which will better define the solar lines in this region compared to the nominal case where the intensity level is low at the ends (case of the image for the central part for example). The same remark is valid for the end of the green curve corresponding to the third part of the order spectral band where an improvement is also expected.

The next step now is to extract the spectral band parts that will be assembled. This starts first by calculating the 2 abscissa (wavelengths) corresponding to the intersection of the blue-red curves then that of the red-green curves (see Figure 11 at the top). The first part of the spectral band will correspond to the blue curve up to the first intersection between the blue and red curves: this is the left part. The second part is the red curve taken between the 2 intersections: this is the central part. Finally, the third part is the green curve taken from the second intersection between the red and green curves to the end: this is the right part. The left, central and right parts form the combined spectral band of diffraction order 101, which is not contaminated. It is plotted in black in Figure 11 at the bottom.

The last step in the process of assembling the curve parts consists of correcting the combined spectral band for variations x in intensity, each curve part being well approximated by a Blaze function as seen in Section 3.1. An improvement of the continuum fixed at 1 is then carried out as explained in Section 3.1. Figure 12 plots the final result obtained for the spectral band of order 101 (red curve) with the corresponding part of the Toon's reference spectrum for comparison (green curve). A very good agreement is observed between the two spectra. No additional solar lines due to contamination are visible at the ends of the spectral band of order 101 obtained from the combination.

Figure 13 at the top also plots for comparison the spectral band of order 101 from the combination method with that obtained from the geometric method. We can see that the spectral band resulting from the combination gives better results. Indeed, we can notice that the solar lines are deeper but also better resolved (see bottom

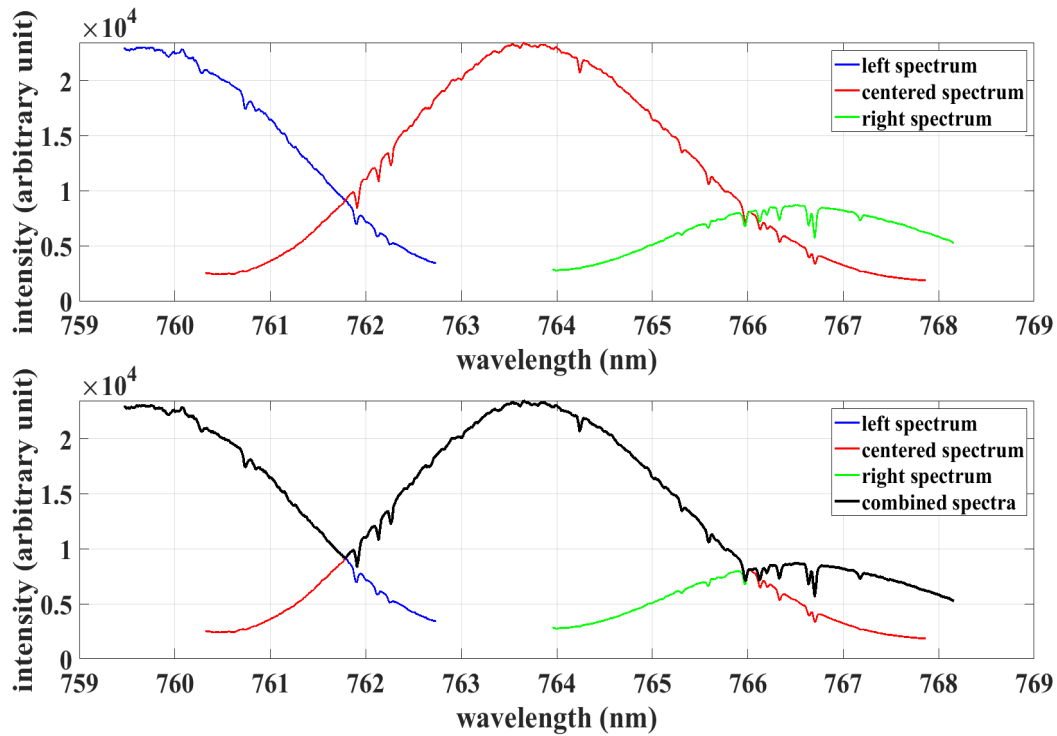


Figure 11. Top: Spectral bands obtained from images of the diffraction order 101. Bottom: The parts of the spectral bands are combined to reconstruct a new one without spectral contamination of the order 101.

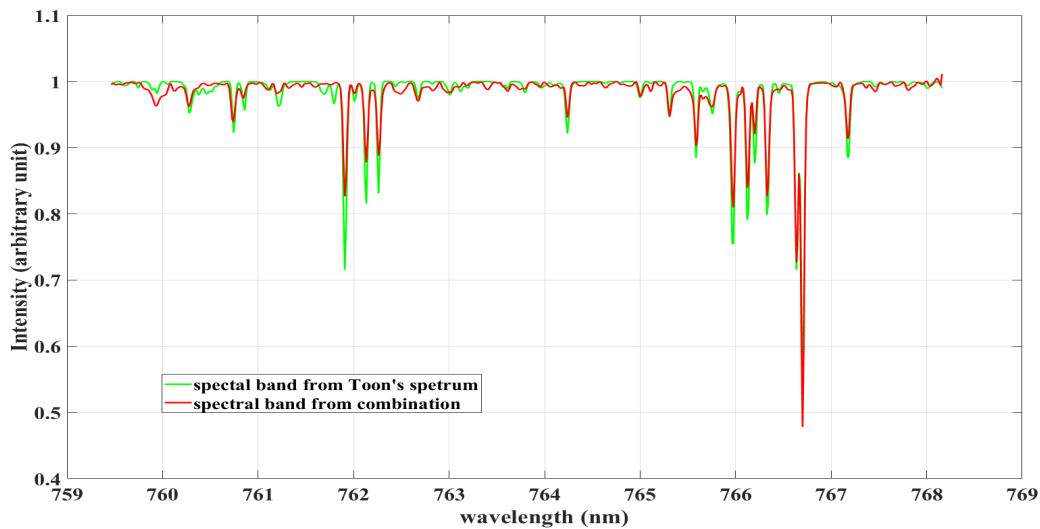


Figure 12. The spectral band of diffraction order 101 obtained with the combination method (red) and the Toon's reference spectrum (green).

plot in Figure 13). Figure 14 plots the same type of curves as figure 13 but for the spectral band of order 98. The bottom graph which zooms in on the spectral band shows better results with the combination method regarding the detection of solar lines at the end of the spectral band.

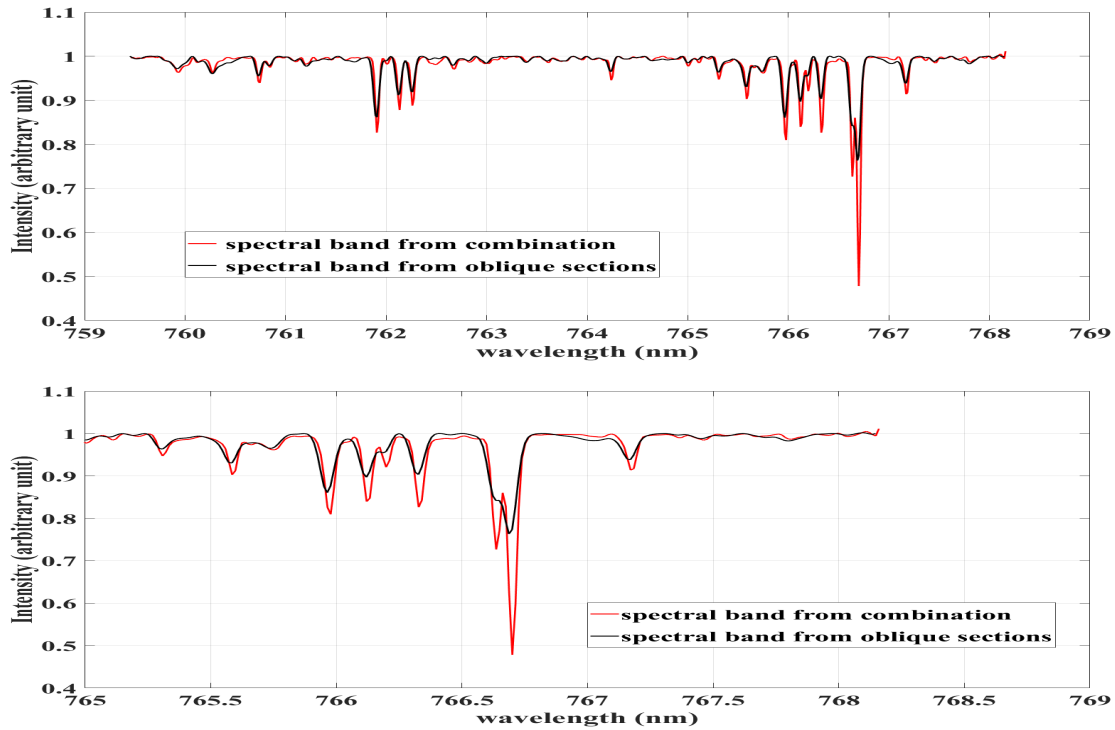


Figure 13. Top: Spectral band of diffraction order 101 obtained by the combination (red) and geometric (black) methods. Bottom: zoom on the spectral band showing the best quality obtained with the combination method.

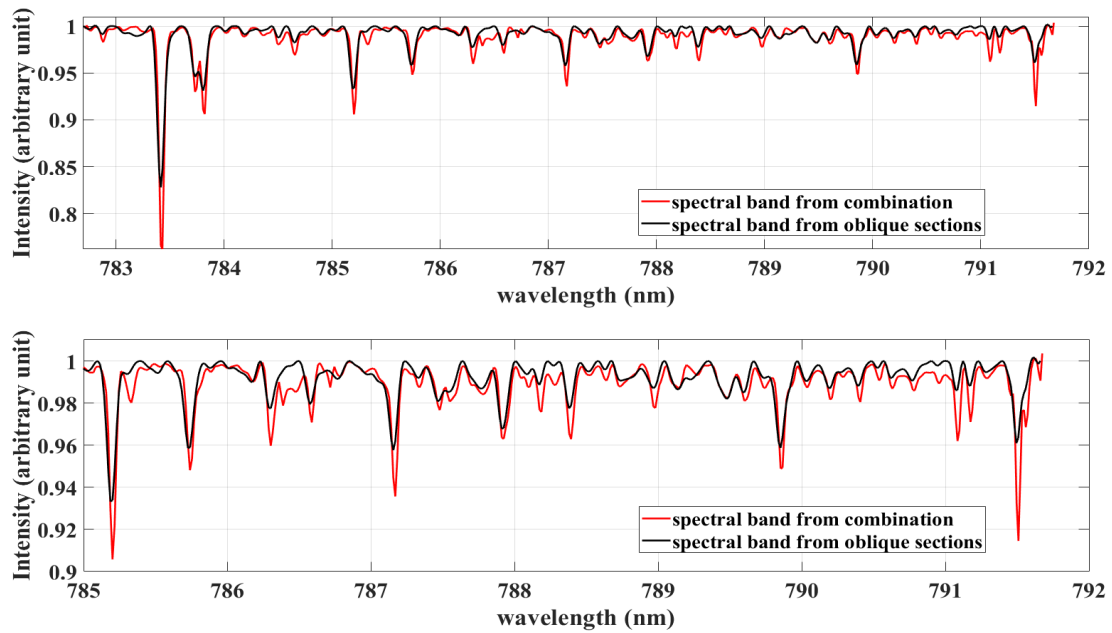


Figure 14. Top: Spectral band of diffraction order 98 obtained by the combination (red) and geometric (black) methods. Bottom: zoom on the spectral band showing better detection of solar lines at the end of the spectral band.

4.2 The solar spectrum obtained from the combination method

The combined method is now used to process all ACS-NIR diffraction orders in order to calculate the solar spectrum over the range allowed by the spectrometer, i.e. from 0.7 to 1.7 μm with some inaccessible spectral gaps due to the optical concept of the instrument (see Section 2.1). The solar spectrum is obtained in the case where the integration region considered is the whole Sun (see Section 3.1). The result is shown in Figure 15 at the top where the black curve is the solar spectrum in its final version obtained with ACS-NIR. The green curve is the Toon's solar spectrum, which serves as a reference to compare the one we obtained with ACS-NIR (see Section 2.3). A very good overall agreement is observed between the ACS-NIR spectrum and that of Toon. The bottom plot of the figure 15 zooms in on diffraction orders 80, 79 and 78 (from left to right) of the ACS-NIR taken arbitrarily to judge a closer comparison with the Toon spectrum. This confirms that the 2 spectra are very close. The overall agreement between the ACS-NIR and Toon spectra is best appreciated when represented as images in Figure 16 (top) where each line is the spectral band of a diffraction order.

However, looking closer by zooming in on the two images around orders 52 to 59 (see the middle images in Figure 16), we clearly see a difference in this band. Indeed, there are solar lines present in the ACS-NIR spectrum (right image) but not in the Toon reference spectrum (left image). This is even better visible in

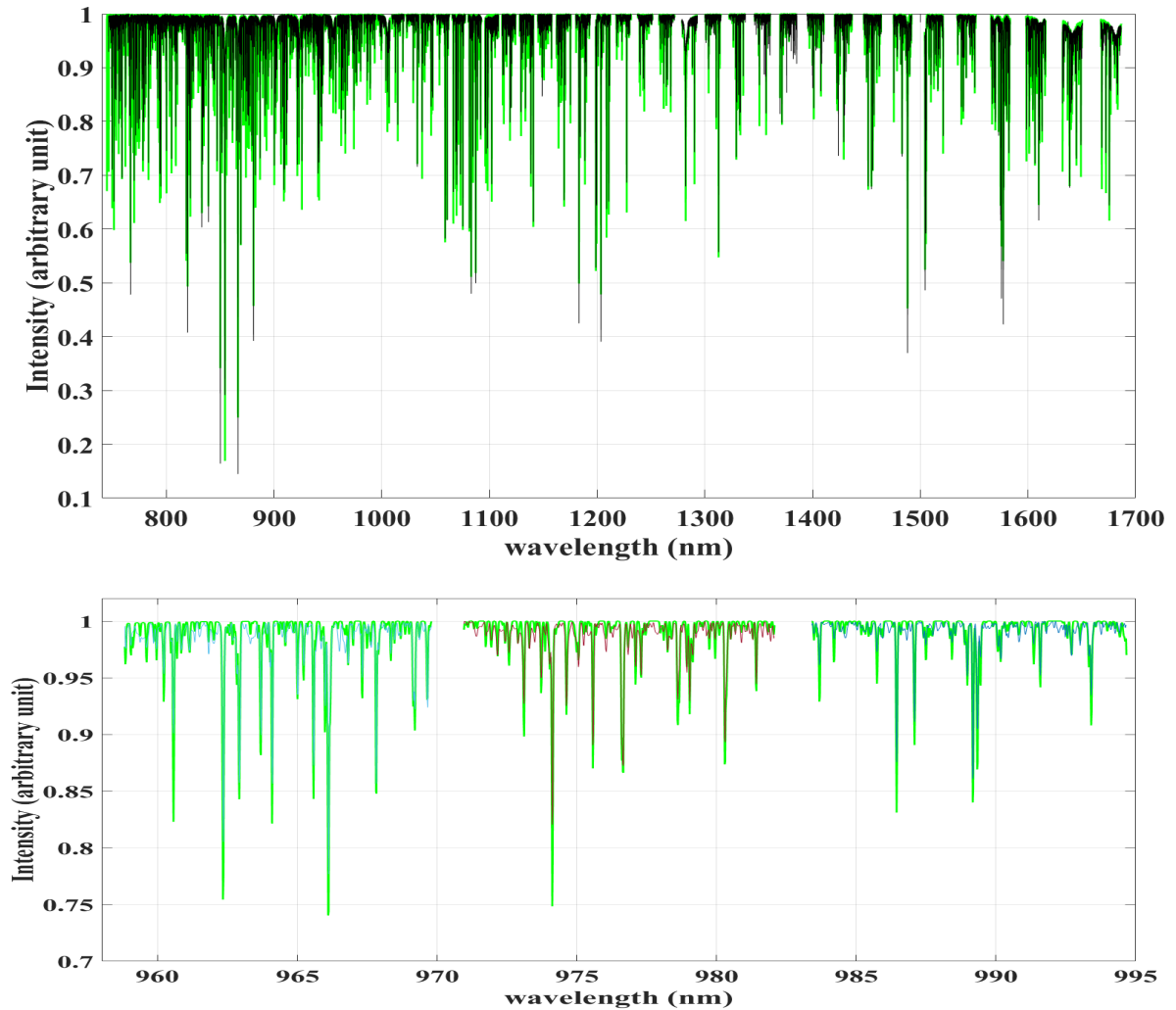


Figure 15. Top: Solar spectrum obtained from ACS-NIR using the order combination method (black) and the Toon reference one (green). Bottom: The spectral bands of orders 80, 79 and 78 showing good agreement with the reference.

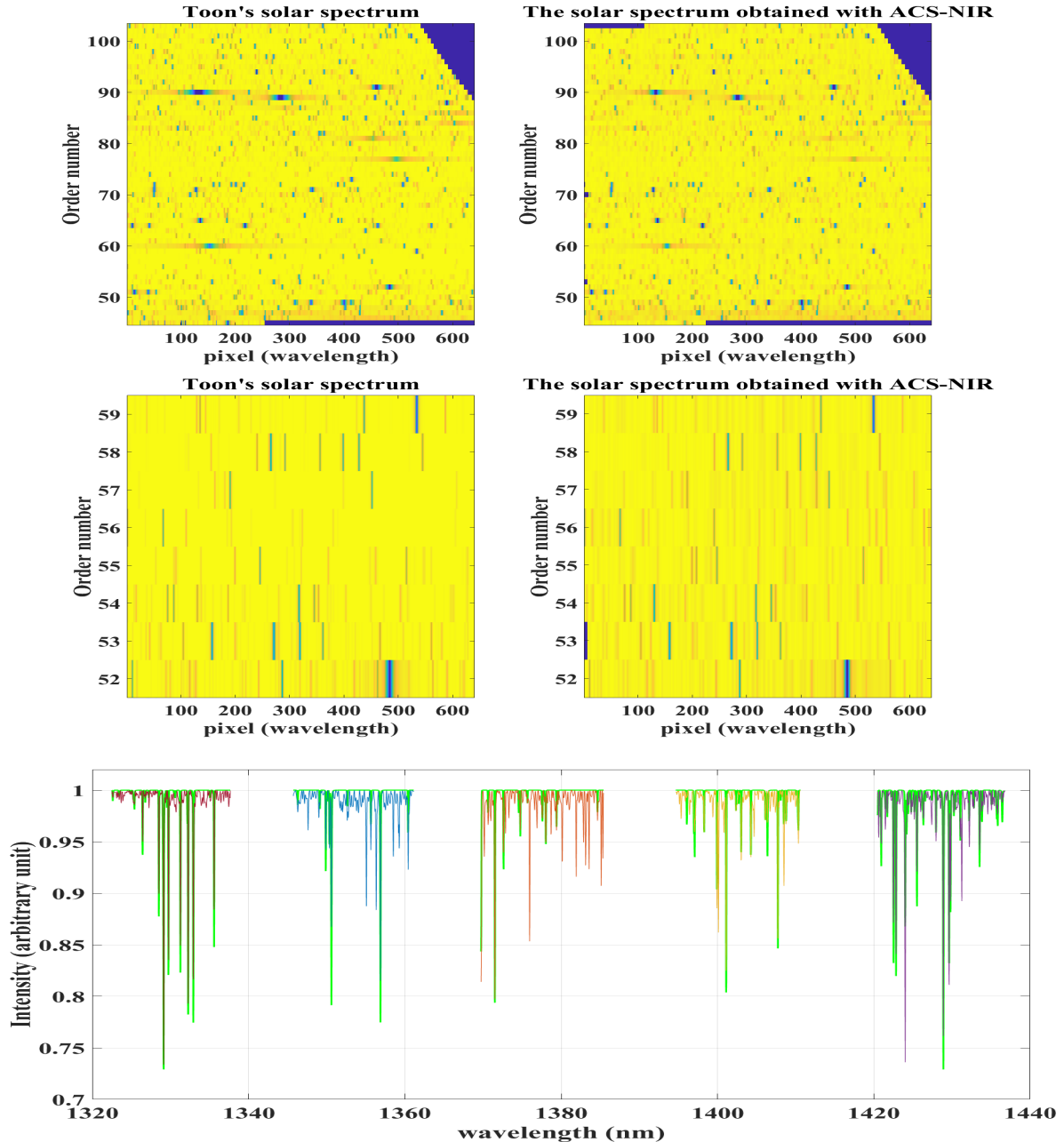


Figure 16. Top: Toon solar spectrum (left) and that obtained with ACS-NIR. Each image line is the spectral band of a diffraction order. Middle: Zoom on the top images between orders 52 and 59: a difference is clearly visible. Bottom: A zoom on the two spectra from orders 54 to 58 (from left to right) shows solar lines in the ACS-NIR spectrum that are not present in that of Toon.

Figure 16 at the bottom where the spectral bands of the orders 54 to 58 are represented as a function of wavelength. The discovery of these *new spectral lines* was only possible thanks to space spectrometry, that is to say by overcoming the forbidden infrared windows of the Earth's atmosphere imposed essentially by its water content. Indeed, the Toon reference spectrum is constructed from ground and balloon observations corrected for atmospheric transmission with a model calculated using HITRAN (see Section 2.3). The forbidden windows of the atmosphere do not allow measurements with ground-based spectrometers in these infrared bands, thus making the reconstruction of these parts of the spectrum impossible.

ACS-NIR measurements to obtain the solar spectrum were carried out during periods of low solar activity (see Section 2.2.2). The open question is whether the same spectral or other lines still exist during periods of highest solar activity. An observation program will be requested soon in response to reacquire the diffraction orders which show these new lines.

5. CONCLUSION

Knowledge of the solar spectrum at high spectral resolution is fundamental for studies of the Sun or for space missions probing the atmospheres of the planets in our solar system (Earth, Mars, etc.). It is indeed very useful for the latter for the calibration of atmospheric spectra measured with on-board instruments. The infrared parts of the solar spectrum currently used were obtained from ground observations corrected for atmospheric transmission but this is a difficult exercise outside the observation windows permitted by the Earth's atmosphere. However, there are sometimes opportunities to measure the solar spectrum at high resolution in space. This is the case of the TGO space mission launched in 2016 and currently in orbit around Mars. It carries on board the NIR spectrometer mounted on the ACS platform and used to probe the Martian atmosphere. The solar spectrum can, however, be obtained in observations when it is pointed toward the Sun and its line of sight is above the atmosphere. Thus, calibration data were carried out for around ten months in 2020-2021 for this purpose but also to study the instrumental effects of the spectrometer ACS-NIR which affect the measurements. The objective of measuring the solar spectrum was the subject of a first study presenting a geometric method which uses all the calibration data to generate a first version of the spectrum.⁴ The instrumental properties of the ACS-NIR were then studied taking advantage of the previous study to establish the spectral contamination matrix which defines how successive diffraction orders are contaminated.⁹ These two studies are summarized in this paper because they serve to define the new method for the final estimation of the solar spectrum by overcoming the limits of the geometric method. This new method uses three images of the same diffraction order acquired with different frequencies of the AOTF (Acousto-Optic Tunable Filters) of ACS-NIR. They are chosen and extracted from the calibration data. An uncontaminated part is extracted from each of the 3 images thanks to the spectral contamination matrix. They are then combined to reconstruct the spectral band of the diffraction order. This reconstruction process firstly makes it possible to avoid cross-contamination of the diffraction orders and to improve the detection of solar lines where the intensity is low at the ends of the order image. Secondly, it also avoids interpolations in the image of order spectral bands needed for the geometric method⁴ and consequently filtering in the solar spectrum. The method was first applied in this article to diffraction order 101 taken as a typical example because it is likely to exhibit spectral contamination. The results obtained were discussed with regard to the improvements made compared to the geometric method (contamination, filtering and detection of solar lines at low intensity levels). They showed that the spectral band obtained was not contaminated by its neighbors and that it was of better quality compared to that calculated with the geometric method.

The new method was then extended to handle all ACS-NIR diffraction orders and the results compared to the Toon's reference spectrum.^{2,7} They were presented and discussed in this paper showing an undeniable improvement in the solar spectrum obtained. The results also clearly show that there are solar lines present in the ACS-NIR spectrum but not in the Toon's reference spectrum. The discovery of these *new spectral lines* was only possible thanks to space spectrometry, that is to say by overcoming the forbidden windows imposed essentially by the water content of the Earth's atmosphere. Indeed, the infrared windows prohibited in the atmosphere do not allow measurements with ground-based spectrometers in these bands.

In summary, the final version of the solar spectrum which will be published soon is the one obtained using this new method presented.

The ACS-NIR observations allowing this version of the solar spectrum were carried out during periods of low solar activity (2020-2021). Do the same or other spectral lines exist during higher solar activity? An observation program will be requested soon to answer the question.

The method has the advantage of using only a few image pieces (3) per diffraction order. It can then be used in ACS-NIR nominal mode without increasing the telemetry when probing the Martian atmosphere, thus avoiding any contamination between diffraction orders.

REFERENCES

- [1] Vial, J.-C., [[1. Le Soleil, une étoile dans notre Galaxie In : Le ciel à découvert \[inline\]](#)], Paris : CNRS Éditions (2010).
- [2] Toon, G. C., “Solar line list for the tcon 2014 data release,” (2015).
- [3] Korablev, O., Montmessin, F., Trokhimovskiy, A., Fedorova, A., Shakun, A., Grigoriev, A., Moshkin, B., Ignatiev, N., Forget, F., Lefèvre, F., Anufreychik, K., Dzuban, I., Ivanov, Y., Kalinnikov, Y., Kozlova, T., Kungurov, A., Makarov, V., Martynovich, F., Maslov, I., Merzlyakov, D., Moiseev, P., Nikolskiy, Y., Patrakeev, A., Patsaev, D., Santos-Skripko, A., Sazonov, O., Semena, N., Semenov, A., Shashkin, V., Sidorov, A., Stepanov, A., Stupin, I., Timonin, D., Titov, A., Viktorov, A., Zharkov, A., Altieri, F., Arnold, G., Belyaev, D., Bertaux, J., Betsis, D., Duxbury, N., Encrenaz, T., Fouchet, T., Gérard, J., Grassi, D., Guerlet, S., Hartogh, P., Kasaba, Y., Khatuntsev, I., Krasnopolsky, V., Kuzmin, R., Lellouch, E., Lopez-Valverde, M., Luginin, M., Määttänen, A., Marcq, E., Torres, J., Medvedev, A., Millour, E., Olsen, K., Patel, M., Quantin-Nataf, C., Rodin, A., Shematovich, V., Thomas, I., Thomas, N., Vazquez, L., Vincendon, M., Wilquet, V., Wilson, C., Zasova, L., Zelenyi, L., and Zorzano, M., “The atmospheric chemistry suite (acs) of three spectrometers for the exomars 2016 trace gas orbiter,” *Space Science Reviews* **214**(1) (2018).
- [4] Irbah, A., Bertaux, J.-L., Montmessin, F., Scheveiler, L., Lacombe, G., Trokhimovskiy, A., Korablev, O., Fedorova, A., Patrakeev, A., and Shakun, A., “Processing of ACS-NIR observations to build the solar spectrum with high spectral resolution in the 0.7-1.7 μm domain,” in [[Space Telescopes and Instrumentation 2022: Optical, Infrared, and Millimeter Wave](#)], Coyle, L. E., Matsuura, S., and Perrin, M. D., eds., **12180**, 121803H, International Society for Optics and Photonics, SPIE (2022).
- [5] Irbah, A., Bertaux, J.-L., Montmessin, F., Scheveiler, L., Rouanet, N., Trokhimovskiy, A., Korablev, O., and Fedorova, A., “New methods for estimating flat field and stray light images from the ACS-NIR spectrometer on board TGO,” in [[Proceedings of the Conference on 'Smart Sensors and Systems: Technology and Applications \(SSS&TA' 2022\)](#)], (2022).
- [6] Hestroffer, D. and Magnan, C. N., “Wavelength dependency of the solar limb darkening,” *Astronomy and Astrophysics* **333**, 338–342 (1998).
- [7] Toon, G. C., “The solar spectrum: An atmospheric remote sensing perspective,” (2013).
- [8] Gordon, I., Rothman, L., Hill, C., Kochanov, R., Tan, Y., Bernath, P., Birk, M., Boudon, V., Campargue, A., Chance, K., Drouin, B., Flaud, J.-M., Gamache, R., Hodges, J., Jacquemart, D., Perevalov, V., Perrin, A., Shine, K., Smith, M.-A., Tennyson, J., Toon, G., Tran, H., Tyuterev, V., Barbe, A., Császár, A., Devi, V., Furtenbacher, T., Harrison, J., Hartmann, J.-M., Jolly, A., Johnson, T., Karman, T., Kleiner, I., Kyuberis, A., Loos, J., Lyulin, O., Massie, S., Mikhailenko, S., Moazzen-Ahmadi, N., Müller, H., Naumenko, O., Nikitin, A., Polyansky, O., Rey, M., Rotger, M., Sharpe, S., Sung, K., Starikova, E., Tashkun, S., Auwera, J. V., Wagner, G., Wilzewski, J., Wcisło, P., Yu, S., and Zak, E., “The hitran2016 molecular spectroscopic database,” *Journal of Quantitative Spectroscopy and Radiative Transfer* **203**, 3–69 (2017). HITRAN2016 Special Issue.
- [9] Irbah, A., Bertaux, J.-L., Montmessin, F., Scheveiler, L., Lacombe, G., Rouanet, N., Trokhimovskiy, A., Korablev, O., and Fedorova, A., “Spectral contamination between diffraction orders of the NIR spectrometer (TGO) but possible solutions to overcome it,” in [[Society of Photo-Optical Instrumentation Engineers \(SPIE\) Conference Series](#)], Minoglou, K., Karafolas, N., and Cugny, B., eds., *Society of Photo-Optical Instrumentation Engineers (SPIE) Conference Series* **12777**, 127776Z (July 2023).